INTERNATIONAL SOCIETY FOR
SOIL MECHANICS AND
GEOTECHNICAL ENGINEERING

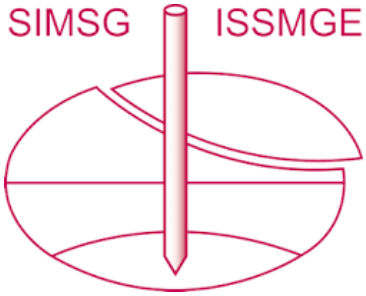

This paper was downloaded from the Online Library of the International Society for Soil Mechanics and Geotechnical Engineering (ISSMGE). The library is available here:

https://www.issmge.org/publications/online-library

This is an open-access database that archives thousands of papers published under the Auspices of the ISSMGE and maintained by the Innovation and Development Committee of ISSMGE.

Geotechnical Aspects of Underground Construction in Soft Ground – Viggiani (ed)
© 2012 Taylor & Francis Group, London, ISBN 978-0-415-68367-8

Numerical analysis of 20.5 m deep excavation with anchored diaphragm wall

J. Josifovski, S. Gjorgjevski & M. Jovanovski
Faculty of Civil Engineering-Skopje, University Ss. Cyril and Methodius, R. Macedonia

ABSTRACT: The deep excavation in built-up urban areas surrounded by high-rise buildings with deep basements makes this engineering problem quite formidable. Such a project for construction of eight storey administrative-residential building located in the city centre of Tirana, Albania is described in this paper. It anticipates a 20.5 m deep excavation surrounded by six and eight storey buildings with basements. To ensure an undisturbed excavation of 27.7 × 36.9 m pit a multi anchored diaphragm wall has to be constructed. The finite element method has been used to check the stability, calculate the system and determine the internal forces, displacements, support reactions under earth and water pressure. The proposed model had been able to give realistic estimation of the excavation soil behaviour which was proved during the process of construction.

1 INTRODUCTION

The excavation of 27.7 × 36.9 m pit is necessary for construction of eight storey administrative-residential building in the city centre of Tirana. The structure has six underground storeys with bottom floor as a basement, next 3 floors as parking lots while the top 2 floors are shopping and administrative premises. All together sums up to a depth of 20.5 m, see Figure 1.

The excavation is secured by diaphragm wall with thickness $t = 0.8$ m, length $L = 129.2$ m and height $H = 25$ m which has only a temporal character. The reinforced concrete wall is constructed out of segments with 2.7 m width. The supporting structure represents a multi anchored diaphragm wall with height of 20.5 m plus additional 4.5 m depth bellow the pit. The supports are pre-stress anchors introducing additional stabilizing forces in the system. Depending on the requirements anchor type TTS15 with 5, 6 and 7 cables has been employed. Every cable is comprised out of 7 wires ϕ5 mm with total diameter of 15 mm. The horizontal anchor spacing is $L_s = 2.7$ m and vertical is $h_s = 3$ m. The anchors are positioned with inclination of 15 degrees to the horizontal and varying length.

2 CONSTRUCTION PROCEDURE

The excavation had been performed according to carefully devised procedure. To ensure a safe excavation of the pit, first a diaphragm wall has to be constructed. Specialized machines were employed to excavate the wall. After positioning of reinforcement a continuous concrete pour through fixed pipes has been executed is 25 m deep. The construction of the diaphragm wall enabled the next phase, namely the excavation of the pit. The excavation and positioning of the anchors has been performed in six continuous phases which are described in Table 1 with respect to the excavation depth h.

Parallel to the excavation a dewatering of the pit had been performed using pumps with sufficient capacity and number. The anchoring is performed in counter-clockwise direction with rotational drilling and piping (130–180 mm). Next the grouting if the anchors is performed using a cement injection mass with 3% bentonit. After reaching the hardening condition of the injection mass the pre-tensioning of the anchors can start. Before proceeding with the excavation of the next phase the anchors from the previous have to been finished. To ensure that design values of the anchor forces are properly introduced it is necessary that 10% of anchors fulfil the acceptance test.

3 GROUND CONDITIONS

The boreholes gave a clear picture of the ground profile which is comprised out of 10 almost horizontal layers. The ground conditions in this project were defined according to data obtained from the field investigations and laboratory tests.

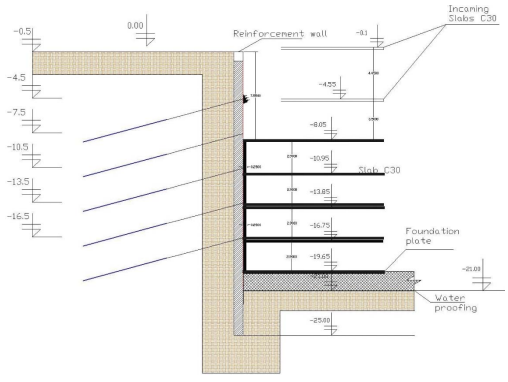

Figure 1. Multi anchored diaphragm wall section AA(left) protecting the excavation.

Table 1. Excavation phases.

Phase	1	2	3	4	5	6
h (m)	–4.0	–8.0	–11.5	–14.5	–17.5	–20.5

Table 2. Soil properties.

Type	h (m)	γ (kN/m^3)	ν (*I*)	M_v (MPa)	c (kPa)	ϕ (^{0})
N	1.0	17.0	0.3	3	5	18
CI	3.4	19.3	0.3	10	30	18
ML	5.9	19.1	0.31	8	10	20
GW	6.8	19.0	0.34	11	25	18
ML	14.5	19.6	0.32	11	15	21
CL	16.0	19.6	0.30	12	5	24
CL	17.5	20.0	0.28	18	45	25
M	20.0	22.0	0.27	25	150	30
M	24.0	24.0	0.26	45	200	32
M	40.0	24.0	0.26	55	250	34

In the numerical model the soil had been represented by the following material parameters: γ as a unit weight, ν as a Poisson's ratio, M_v as a compression modulus, strength parameters c as cohesion and ϕ as angle of internal friction. They are presented in Table 2 for every lithological unit with respect to the depth h.

The top layer (N) is a man-made embankment brownish silty clay containing pieces of bricks and roots with a thickness of 0.7 m; layer (CI) is silty clay mixture with yellow colour medium dense with average thickness of 2.4 m; layer (ML) is clayly silt predominate brown colour medium-dense with thickness from 2.0 to 2.5 m; layer (GW) is sandy gravel with local presence of claylike matrix with thickness of 0.5 m to 0.7 m; layer (CL) is composed of silty clay mixtures medium low dense yellow colour encountered at 4.5 up to 9 m depth; layers (M) are Neogene's deposits composed by claylike Marls to highly weathered alveoli. The underground water is present on 4 to 5 m below ground surface in layers (ML) and (GW) while top and bottom layers are with low permeability and relatively dry.

4 NUMERICAL ANALYSIS

In order to obtain a realistic behaviour of the deep excavation supported by a diaphragm wall the problem has been analysed with the finite element method. The computer program Plaxis which is specialized for geotechnical engineering has been used in combination with some analytical solutions. The program enables simple but efficient spatial modelling of different structural elements and accurate material definition.

The ground stress-strain state during excavation is calculated on a two-dimensional plane-strain finite element model. The soil is discretized as elastoplastic material using a Mohr-Coulomb definition vis-a-vis the reinforced concrete wall as a linear material. The spatial discretization had been varied depending on the situation and detailing level but in general triangular plane elements with 15 nodes had been used. The structural elements were modelled using three node beam elements.

4.1 *Excavation*

Since there is a difference in the ground and loading conditions on the construction site it was decided that all four sides of the pit has to be analysed. The excavation pit from three sides is surrounded by buildings with basements, thus different structural solutions of the anchored diaphragm wall are necessary. They are distinguished by the wall section name e.g. AA or BB followed by subscripts 'l' or 'r' for left and right side. The stage construction has been simulated in six continuous phases, hence the initial phase calculates the initial ground stresses with constructed diaphragm wall. The excavation scenario from Table 1 is illustratively presented in Figure 2.

First, a finite element analysis with fix-end anchors has been performed to determine the characteristic force for every phase in different level. The results for both wall sections left to right are presented in Table 3 through Table 6.

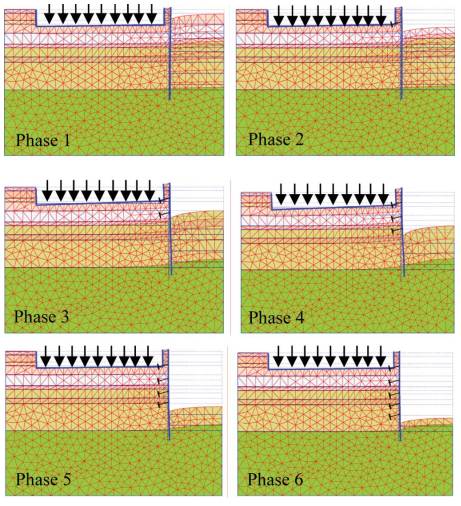

Figure 2. Deformed finite element mesh of wall section AA_l for construction phase (1–6).

Table 3. Characteristic phase anchor force in wall section AA_1.

	P_k (kN/m)				
Level (m)	Ph.2	Ph.3	Ph.4	Ph.5	Ph.6
–4.0	240.3	146.2	155.1	158.0	164.7
–8.0		541.8	493.6	491.2	492.2
–11.5			401.2	422.4	417.2
–14.5				401.2	502.5
–17.5					470.5

Table 4. Characteristic phase anchor force in wall section AA_r.

	P_k (kN/m)				
Level (m)	Ph.2	Ph.3	Ph.4	Ph.5	Ph.6
–4.0	194.7	79.4	80.6	79.6	87.9
–8.0		501.7	449.2	448.4	451.6
–11.5			372.8	385.3	381.1
–14.5				382.4	428.4
–17.5					401.1

The calculation of the required anchor forces is performed with respect to the overall stability in every phase of excavation.

4.2 *Anchors*

The anchor lock-off force P_0 has been determined according to EN 1537 as.

$$P_0 = 0.60 P_{tk} \quad (1)$$

Table 5. Characteristic phase anchor force in wall section BB_l.

	P_k (kN/m′)				
Level (m)	Ph.2	Ph.3	Ph.4	Ph.5	Ph.6
–4.0	–	–	–	–	–
–10.5		134.0	26.0	34.4	42.8
–11.5			495.9	480.0	467.1
–14.5				355.4	372.0
–17.5					361.2

Table 6. Characteristic phase anchor force in wall section BB_r.

	P_k (kN/m′)				
Level (m)	Ph.2	Ph.3	Ph.4	Ph.5	Ph.6
–4.0	199.4	87.8	92.6	93.5	99.8
–8.0		533.3	479.5	479.8	482.6
–11.5			396.7	404.0	400.0
–14.5				432.3	474.2
–17.5					459.5

Table 7. Lock-off tendon force.

Anchor type	P_0 (kN)	P_0/L_a (kN/m)
4TTS15	840	311
5TTS15	1050	389
6TTS15	1260	467
7TTS15	1470	544

where P_{tk} is the characteristic load capacity of tendon. In the case of TTS15, $P_{tk} = 350$ kN, which leads to 210 kN as loading capacity per anchor thread. The total tendon force is assumed to be N (number of cables) times the thread force, see Table 7.

According these values adequate anchor types have been assumed which fulfil minimum required force P_k for different sections of the wall, see in Table 8 through Table 11.

4.3 *Anchor grouted body*

A special attention had been given to the calculation of a single anchor following the classical solution after P. Lendi, see Figure 5.

The grouted body of the anchor is positioned in the layer (M)—Marls (below depth 10.5 m) with

Table 8. Anchors in wall section AA_l.

Level (m)	Anchor type	P_0 (kN/m)	P_0 (kN)
–4.0	4TTS15	311	840
–8.0	7TTS15	544	1470
–11.5	6TTS15	467	1260
–14.5	7TTS15	544	1440
–17.5	6TTS15	467	1260

Table 9. Anchors in section AA_r.

Level (m)	Anchor type	P_0 (kN/m)	P_0 (kN)
–4.0	4TTS15	311	840
–8.0	7TTS15	544	1470
–11.5	5TTS15	389	1050
–14.5	6TTS15	467	1260
–17.5	6TTS15	467	1260

Table 10. Anchors in wall section BB_l.

Level (m)	Anchor type	P_0 (kN/m)	P_0 (kN)
–4.0	–	–	–
–10.5	4TTS15	311	840
–11.5	6TTS15	467	1260
–14.5	5TTS15	389	1050
–17.5	5TTS15	389	1050

Table 11. Anchors in wall section BB_r.

Level (m)	Anchor type	P_0 (kN/m)	P_0 (kN)
–4.0	4TTS15	311	840
–8.0	7TTS15	544	1470
–11.5	6TTS15	467	1260
–14.5	6TTS15	467	1260
–17.5	6TTS15	467	1260

anchor bond length at L_b = 15 m. The calculation determines many important parameters e.g. design resistant anchor force $R_d = R_k / \gamma_R$ of where γ_R is a partial factor of anchor resistance, see Table 12.

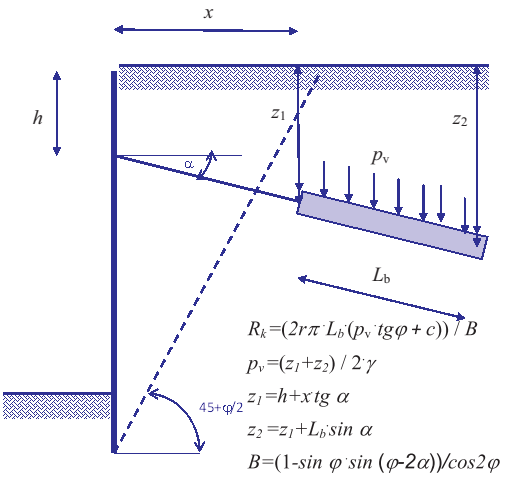

Figure 5. Ground anchor.

Table 12. Soil and anchor properties.

Cohesion	c	150	kPa
Internal friction	ϕ	30°	0.523
Unit weight	γ	19.2	kN/m^3
Height	H	11.5	m
Distance	x	10.0	m
Bond length	L_b	15.0	m
Angle to horizontal	α	15°	0.262
Width	B	1.3	m
Start depth	z_1	14.18	m
End depth	z_2	18.06	m
Earth pressure	p_v	309.52	kPa
Resistance force	R_k	2323.44	kN
Partial factor	γ_R	1.35	/
Design resistant force	R_d	1721.06	kN

A more comprehensive analysis with greater detailing and application of so-called node-to-node anchors has been performed next, see Figure 6.

Using this type of anchors, comprised of tendon and grouted body, should help to obtain more realistic picture of the stress distribution of the anchors in the soil. In this model the anchors have been prestressed with the determined lock-off force from Table 4. The program calculates the problem which to a solution of the displacements, see Figure 7.

The maximal displacements in the soil are in the layer GW close to the grouted bodies between the second and third anchor. The displacements are around 4 cm with no implications on the stability of the wall.

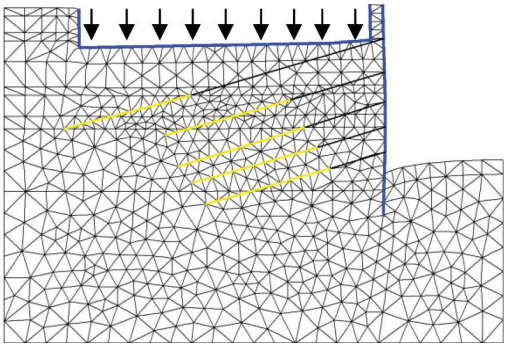

Figure 6. Deformed finite element mesh of wall section AA_l (phase: 6).

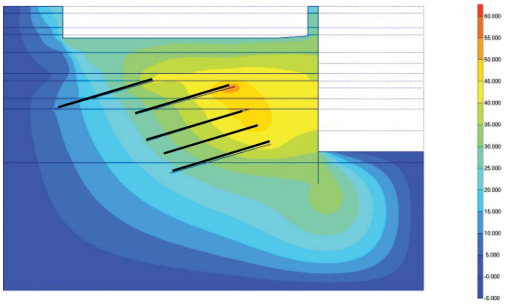

Figure 7. Horizontal displacements of wall section AA_l (phase 6: shadings).

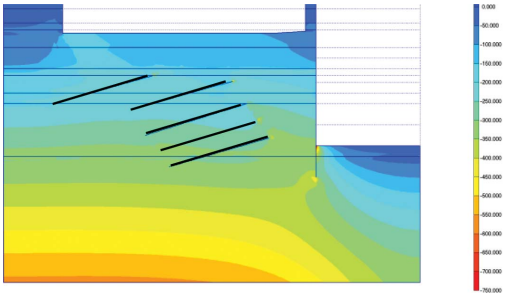

Figure 8. Effective stresses of wall section AA_l (phase 6: mean shadings).

The soil displacements are result of the stress distribution in the ground, therefore the effective mean stresses is presented in Figure 8.

Slight stress concentration can be seen in the toe of the diaphragm wall which is not significant for the stability. In the soil next to the wall the stress ranges from 150–400 kPa.

Moreover, this calculation can be used to confirm the assumptions made with the analytical solution. Hence, the built-up force in the anchor can be evaluated through a force-displacement relation, see Figure 9.

The ordinate *Sum-Mstage* represents the percentage of the applied anchor force while u_t is the total anchor displacement. At design resistant force P = 1720 kN (or *Sum-Mstage* = 1) the displacement is slightly below 4 cm (in a strain range below 0.3%). The anchors free length L_f is variable depending on the level as it is shown in Table 13.

4.4 *Diaphragm wall*

Beside the soil stress and deformation these analysis also determines the forces and bending moments inside the structural elements. They are presented as cumulatively as envelopes covering all phases of construction. Internal forces and moments of wall section AA_l are presented in Figure 10.

The maximal registered values are: bending moment 388.0 kNm/m, axial force –1370 kN/m and shear force 503.5 kN/m.

Similarly the internal forces and moment for wall section AA_r are presented in Figure 11.

The maximal bending moment is M_{max} = 309.4 kNm/m while maximal internal forces are N_{max} = –1090 kN/m and Q_{max} = 401.2 kN/m.

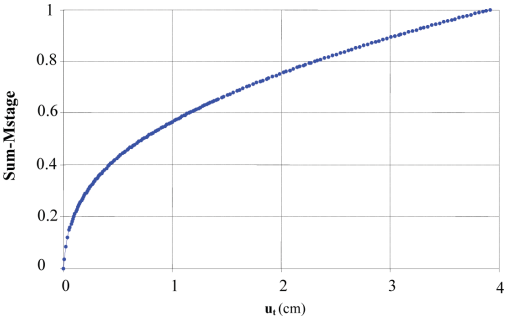

Figure 9. Force-displacement curve of test anchor.

Table 13. Anchors types with total length.

Level (m)	AA_r	AA_l	BB_r	BB_l	$L = L_f + L_b$ (m)
–4.0	4TTS15	4TTS15	4TTS15	–	24.5 + 15
–8.0	7TTS15	7TTS15	7TTS15	–	12.5 + 15
–10.5	–	–	–	4TTS15	11.0 + 15
–11.5	5TTS15	6TTS15	6TTS15	7TTS15	10.5 + 15
–14.5	6TTS15	7TTS15	6TTS15	5TTS15	8.5 + 15
–17.5	6TTS15	6TTS15	6TTS15	5TTS15	7.0 + 15

The envelopes for wall section BB_l are presented in Figure 12.

The maximal bending moment in section BB_l is 641.4 kNm/m, maximal axial force is –743.5 kN/m and maximal shear force is 372.8 kN/m.

Next, envelopes for wall section BB_r are presented in Figure 13.

The maximal bending moment is 416.9 kNm/m, maximal axial force is –1170 kN/m and maximal shear force is 466.5 kN/m.

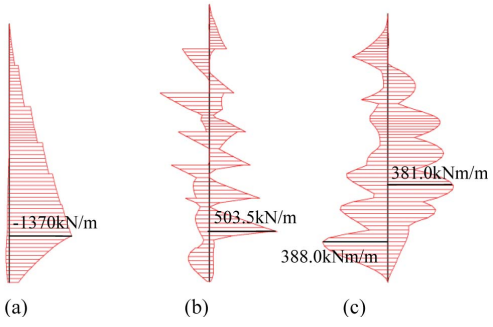

Figure 10. Envelops wall section AA_l: (a) Axial force N, (b) Shear force Q and (c) Bending moment M.

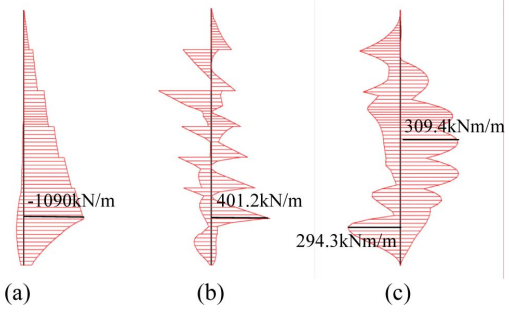

Figure 11. Envelopes in wall section AA_r: (a) Axial forces N, (b) Shear force Q and (c) Bending moment M.

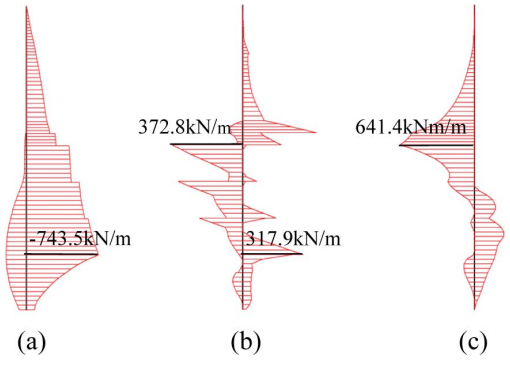

Figure 12. Envelopes in wall section BB_l: (a) Axial force N, (b) Shear force Q and (c) Bending moment M.

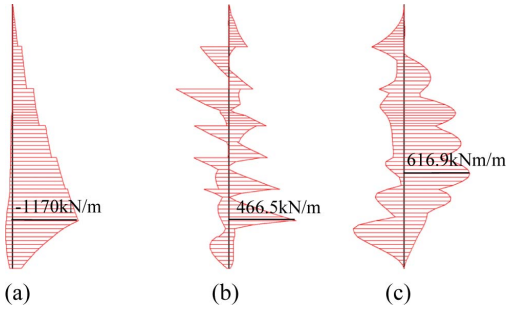

Figure 13. Envelopes in wall section BB_r: (a) Axial force N, (b) Shear force Q and (c) Bending moment M.

Table 14. Maximal internal wall forces and bending moments.

Internal q. vs. wall section	N_{max} (kN/m)	Q_{max} (kN/m)	M_{max} (kNm/m)
AA_l	–1370.0	503.5	388.0
AA_r	–1090.0	401.2	309.4
BB_l	–743.5	372.8	641.4
BB_r	–1170.0	466.5	416.9

Although there are certain differences in the supporting system e.g. anchor force and ground conditions it can be still concluded that there is no large variance in the results. An optimal distribution of the internal forces and moments is obtained which only speaks in favour of the proposed solution, see Table 14.

The wall in section BB_l has the unfavorable load combination due to lowered position of the first row of anchors.

According to these results a design of the reinforced concrete sections of the diaphragm wall had been made according to EN 1992 using the recommended partial factors.

5 CONCLUSIONS

The problem of deep excavation in highly urbanized area such as the city centre of Tirana has proved to be quite formidable engineering task. In particular the greater depth and the built-up surrounding make it especially difficult. In this project a multi anchored diaphragm wall has been used as support to a 20.5 m excavation pit. The paper presents an insight in the process of numerical modelling offering some conclusive discussions.

Several types of analyses had been performed with different level of detailing to help for more

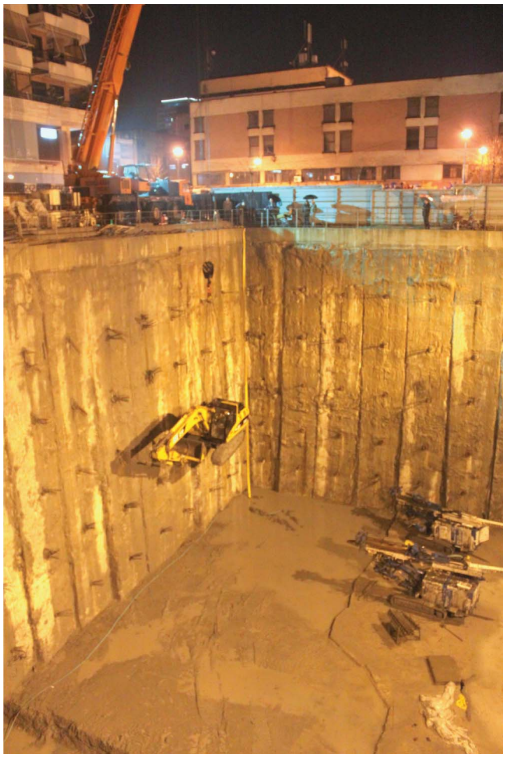

Figure 14. Deep excavation pit with multi anchored diaphragm wall in Tirana.

realistic to simulation of the deep excavation process. Some difficulties of not quite precise regulative were encountered but they were overcome by additional investigations. The proposed numerical model has been able precisely to describe the effects of the anchoring and excavation. The technical solution of multi anchored diaphragm wall had been proved during the actual construction of the wall and excavation of the pit as very effective. At all time the diaphragm wall deflections had been measured. The recordings had confirmed all predictions made in this analysis. The construction had started in September 2009 and finished in March 2010, see Figure 14.

REFERENCES

German Society for Geotechnics (Deutsche Gesellschaft fur Geotechnik e. V.) 2003. Recommendations on Excavations, Ernst & Sohn Verlag fur Architektur und technische Wissenschaften GmbH & Co. KG, Berlin, ISBN 3-433-01712-3.

Kempfert, H.G. & Gebreselassie, B. 2006. Excavations and Foundations in Soft Soils, Springer-Verlag Berlin Heidelberg, ISBN 540-32894-7.

Potts, D.M. & Zdravkovic, L. 1999. Finite element analysis in geotechnical engineering: theory. Imperial College of Science, Technology and Medicine, Thomas Telford Publishing, Thomas Telford Ltd, ISBN 0-7277-2783-4.

Potts, D.M. & Zdravkovic, L. 2001. Finite element analysis in geotechnical engineering: application. Imperial College of Science, Technology and Medicine, Thomas Telford Publishing, Thomas Telford Ltd, ISBN 0-7277-2753-2.

EN 1997–1:1994 Eurocode 7: Geotechnical design—General rules

pr EN 446 Grout for prestressing tendons—Grouting procedures.